Available online at www.sciencedirect.com
SCIENCE DIRECT
Polymer 46 (2005) 1675–1684
polymer
www.elsevier.com/locate/polymer

Formation mechanism of shish in the oriented melt (I)—bundle nucleus becomes to shish

Shinichi Yamazaki[a,*], Kaori Watanabe[b], Kiyoka Okada[b], Koji Yamada[c], Katsuharu Tagashira[c], Akihiko Toda[b], Masamichi Hikosaka[b]

[a]*Faculty of Environmental Science and Technology, Okayama University, 3-1-1 Tsushima-Naka, Okayama 700-8530, Japan*
[b]*Faculty of Integrated Arts and Sciences, Hiroshima University, 1-7-1 Kagamiyama, Higashi Hiroshima 739-8521, Japan*
[c]*R&D Department, Kawasaki Development Center, SunAllomer Ltd, 3-2 Yako 2-chome, Kawasaki-ku, Kawasaki 210-8548, Japan*

Received 21 May 2004; received in revised form 7 December 2004; accepted 7 December 2004
Available online 24 December 2004

Abstract

We have solved the molecular mechanism of the formation of shish of isotactic-polypropylene (iPP) and polyethylene (PE) from the sheared melt based on kinetic study by means of polarizing optical microscope. We found that the rate determining process for the formation of shish is a nucleation process in the most range of degree of supercooling (ΔT) except for large ΔT of PE. We have shown a direct evidence of the formation of bundle nucleus from the oriented melt, which is consisted of elongated chains caused by artificial pins. For polymers, a universal mechanism of nucleation from the isotropic or oriented melt was proposed. We also found that there is a critical shear rate for the formation of shish. This experimental fact indicates that the shish will be formed when the elongation of chains will overcome the conformational relaxation of chains and chain conformation within the oriented melt is kept liquid crystal like one.

Keywords: Nucleation; Shish; Shear flow

1. Introduction

1.1. To solve the crystallization mechanism of polymers under shear flow

Though it is well known that the shish crystals of polymers in the solution or the melt are formed under elongational or shear flow [1–7], no kinetic study to solve the formation and growth mechanisms of shish has been done yet. As well as the study of crystallization of polymers under quiescent state, studies on the crystallization mechanism of polymers under shear flow should be also classified to several stages such as the nucleation, growth and overgrowth. In part 1 of this series of paper, we will solve the formation mechanism of shish under steady shear flow in the initial stage of crystallization. In part 2, we will solve the growth mechanism of shish under continuously shear flow.

1.2. Molecular mechanism and rate determining process of formation of shish

Fig. 1 shows the typical polarizing optical micrographs of crystallization behavior under shear flow. It is to be noted that we can observe both the formation of shish and spherulites at the same experimental condition as shown in Fig. 1(a) [8]. In our previous study, under shear flow with low shear rate $\dot{\gamma}$, we found that the shish was formed from the dust particle within the melt as shown in Fig. 1(b). In low $\dot{\gamma}$, we considered that the formation of shish is not spontaneous but derivative. In our preliminary study, when we attempted to set up the pins on the glass surface of plates on which sandwiches the samples, the shish was effectively formed as shown in Fig. 1(c). Based on our previous experimental facts, we have speculated the chain conformation within the melt under shear flow with low $\dot{\gamma}$

* Corresponding author. Tel.: +81 86 251 8901; fax: +81 86 251 8901.
E-mail address: zaki@cc.okayama-u.ac.jp (S. Yamazaki).

0032-3861/$ - see front matter © 2004 Elsevier Ltd. All rights reserved.
doi:10.1016/j.polymer.2004.12.009

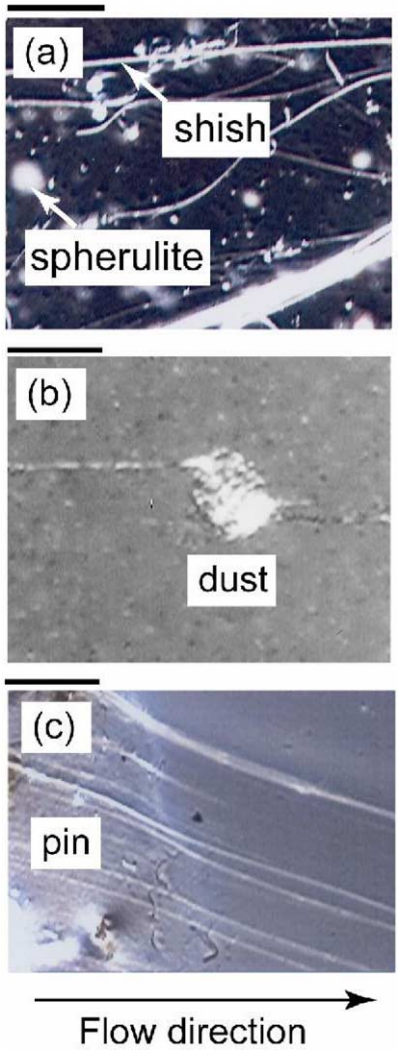

Fig. 1. Typical polarizing optical micrographs of crystallization of iPP under shear flow. (a) Coexistence of spherulite and shish, (b) shish formed from the dust, (c) shish formed from the pins. Scale bar is 50 μm.

(up to ca. 10 s^{-1}) as shown in Fig. 2. The most chains within the sheared melt are not elongated but most chains can be regarded as the ellipsoidal random coils (Fig. 2(A)) as has been reported by small angle neutron scattering (SANS) experiments for the chain conformation under shear flow [9,10] and theoretical study [11,12] or computer simulations [13]. When some chains are accidentally elongated by dusts or pins, the oriented melt will be partially formed in the sheared melt [8]. Therefore, we have to notice that the crystallization from the melt under shear flow with low $\dot{\gamma}$ can be observed from both the isotropic and oriented melt at the same time as shown in Fig. 1(a). We should clearly distinguish the difference between shear and elongational flow [6,7,14]. Needless to say, under elongational flow, most chains will be deformed or extended and the shish will be formed spontaneously.

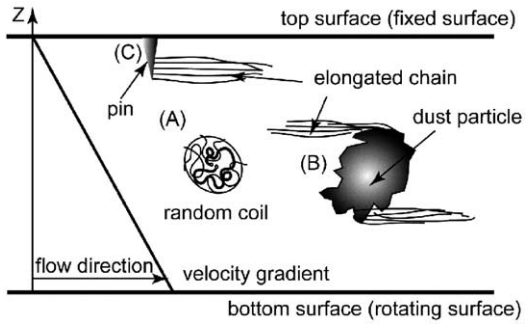

Fig. 2. Schematic illustration of chain conformation within the sheared melt. (A) Ellipsoidal random coil, (B) elongated chains by the dust, (C) elongated chains by the pin.

In polyethylene (PE), we have observed the formation of shish and have proposed the primitive mechanism of formation of shish under shear flow with low $\dot{\gamma}$ [8]. The shish will be formed from the oriented melt caused by dust particles (Fig. 2(B)) or pin of the surface of plates (Fig. 2(C)). First purpose of this work is to confirm the validity of our proposed model under the condition such as low $\dot{\gamma}$ where the chains do not deform or extend. For this purpose, we will show that the number density of shish significantly increases with increase of the number of pins on the surface of plate. Second purpose is to show that the rate determining process for the formation of shish is mainly the nucleation control process not diffusion control process (chain rearrangement). For this purpose, we will determine the degree of supercooling ΔT dependence of the formation rate of shish I_{sh}. It is well known that the nucleation process is a rate process determined by the probability. In other words, the embryo or nucleus will be formed from the original phase with a certain probability due to the fluctuation. This is the same for both homogeneous and heterogeneous nucleations.

1.3. Formation mechanism of spherulite under shear flow

On the other hand, we have also shown that nucleation rate I from the quasi-isotropic melt (ellipsoidal random coils as shown in Fig. 2(A)) obtained by the formation rate of spherulite I_{sp} was almost constant with that under quiescent state [8]. This result means that the formation mechanism of spherulite is essentially the same irrespective of shear flow since the most chains within the sheared melt can be regarded as the ellipsoidal random coils. Since we can consider that the quasi-isotropic melt is included the isotropic melt, we will not distinguish the quasi-isotropic and isotropic melt in this paper.

1.4. Nucleation mechanism and type of nucleus from the oriented and isotropic melt

Fig. 3 shows our proposed universal model of nucleation of polymers from the isotropic and oriented melt. The main feature of our original model is that the different structure of nucleus such as ‘fold and bundle nucleus’ will be formed from the isotropic and oriented melt, respectively. Here, ‘fold and bundle’ mean that chains are folded back at the

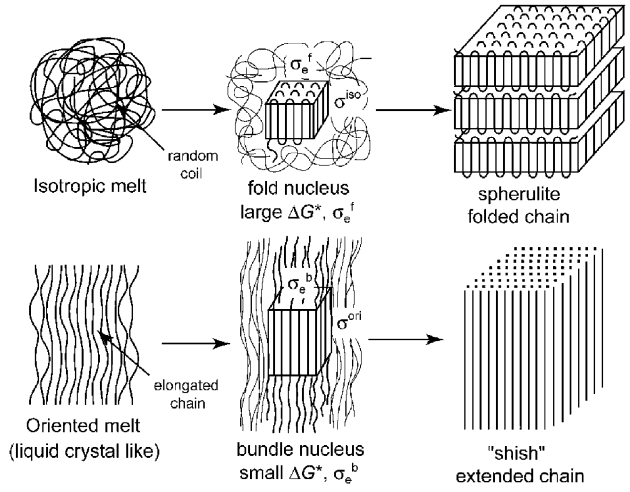

Fig. 3. Schematic illustration of universal model of the nucleation from the isotropic and oriented melt. The spherulite and shish will be formed from the isotropic and oriented melt via fold and bundle nucleus, respectively.

end surface of nucleus and many chains are bound in parallel within the nucleus without fold, respectively. Using the topological nature of polymers such as entanglement and chain sliding diffusion [15,16] arose from long chain molecules, the oriented melt as shown in Fig. 3 can be easily prepared by external fields such as elongation, electric or magnetic fields. According to our model, it is possible to control the type of nucleus such as fold and bundle by controlling the dynamic structure of the melt. In general, it has been accepted for the nucleation of most polymers that the fold nucleus will be formed from the isotropic melt [17]. In the most cases, it is well known that the fold nucleus will grow to spherulite, which is composed stacked lamellar crystals. The extended chain crystal (ECC) [18–20] is formed via significant chain sliding diffusion [15, 16]. On the other hand, though it has been speculated that the bundle nucleus will be formed from the oriented melt [1, 17,21], the formation of bundle nucleus has not been confirmed experimentally yet for polymers. The bundle nucleus will grow to shish, ECCs or fringed micelle crystals [22]. Third purpose is to show the direct experimental evidence that the bundle nucleus is formed from the oriented melt and to confirm the validity of our proposed universal model of nucleation from the oriented and isotropic melt.

1.5. How to judge the type of nucleus

As was shown by Price [17], the type of nucleus such as fold and bundle can be judged from kinetic study. The type of nucleus is definitely reflected the side and end surface free energy (σ and σ_e) included the free energy necessary for forming a critical primary nucleus ΔG^*. According to classical nucleation theory [23,24], I is expressed by

$$I \equiv I_0 \exp(-\Delta G^*/kT) \propto I_0 \exp(-C/\Delta T^2) \quad (1)$$

where k is the Boltzmann constant and T is temperature, I_0 and C are constants. I_0 is proportional to the diffusion constant D and C is proportional to ΔG^*. Here, ΔT is defined by

$$\Delta T = T_m^0 - T_c \quad (2)$$

where T_m^0 is the equilibrium melting temperature and T_c is the crystallization temperature. In the case of homogeneous nucleation, we can obtain the simple relation between ΔG^* and C as, [17]

$$\Delta G^* \propto C/\Delta T^2 \propto \sigma^2 \sigma_e/(\Delta h \Delta T)^2 \quad (3)$$

where Δh is the heat of fusion. Since these equations such as Eq. (1) and (3) are basic and essential, we consider that the complicated treatment reported by Pennings [1] is not necessary. If we can assume that the crystal form of fold nucleus is the same as that of bundle nucleus, we obtain that Δh in the case of the formation of shish is the same as that of the nucleation with fold nucleus. Assuming that the formation of shish is the homogeneous nucleation, we can estimate σ_e for the formation of shish (σ_e^b) using well-known value of C for homogeneous nucleation (C_{homo}) with fold nucleus.

On the other hand, we can obtain σ for the formation of shish (σ^{ori}) independently from ΔG^* of secondary nucleation, i.e. growth rate V of shish. Here, we define that σ^{ori} and σ^{iso} mean σ within the oriented and isotropic melt, respectively. In this paper, we will estimate σ_e^b using σ^{ori} obtained in part 2 of this series of paper [25].

In the case of fold nucleus of PE within the isotropic melt, the σ_e is 7 times as large as σ [26,27]. In the case of small bundle nucleus, it is expected that σ_e is almost the same as σ since there are no foldings on the end surface of nucleus. In other words, the σ_e^b should be much smaller than σ_e^f because the structural difference within the interface of the latter is much larger than that of the former. Though Hoffman et al. pointed out that σ_e^b should be larger than σ_e^f [28], this is only correct when the number of stems within a nucleus becomes large, due to high density of cilia on the end surface. Since we will focus to small nucleus in this work, it is reasonable to regard as $\sigma_e^b \ll \sigma_e^f$ as shown by Price [17]. Therefore, we can judge the type of nucleus from ΔG^*, i.e. ΔG^* of bundle nucleus within the oriented melt is much smaller than that of fold nucleus within the isotropic melt.

1.6. Relaxation of elongated chains and critical shear rate of formation of shish

The elongated chains within the oriented melt caused by pins will relax to random coils. In other words, the entropic relaxation and ordering caused by elongation are competing in all time. It is considered that the chain conformation under shear flow becomes to be a certain elongated state between fully extended and random coil chains. If the formation of shish from the elongated chains within the

oriented melt is the nucleation of bundle nucleus, it is expected that the formation of shish should have a certain critical shear rate $\dot{\gamma}^*$. Because it is necessary that the length of elongated chain should be much larger than the size of critical nucleus. In this work, we will show $\dot{\gamma}^*$ for the formation of shish and propose the model of chain conformation within the sheared melt and the relation between the elongation and relaxation of chains.

1.7. Summary of purpose of this work

We summarized the purpose of this work as below. First purpose is to show that the shish is formed from the oriented melt caused by pins and to confirm that the formation of shish is the nucleation process. Second purpose is to show the direct evidence that the bundle nucleus is formed from the oriented melt. Third purpose is to show that there is $\dot{\gamma}^*$ for the formation of shish. Forth purpose is to propose the model for the elongation and relaxation of chains under shear flow.

2. Experimental

2.1. Samples

The samples used in this work were linear iPP (PM600A supplied by SunAllomer Ltd: $M_w = 25.0 \times 10^4$, $M_w/M_n = 3.57$) and PE (JPE0 supplied by SunAllomer Ltd: $M_w = 11.6 \times 10^4$, $M_w/M_n = 2.42$), where M_w and M_n are weight and number average molecular weights, respectively. In order to characterize our shish obtained by isothermal crystallization under shear flow, we carried out small angle X-ray scattering (SAXS) and wide angle X-ray diffraction (WAXD) measurements. In SAXS and WAXD measurements, the isolated shish was prepared at first as shown in Fig. 1. The sample included the isolated shish was quenched to ambient temperature. Then, the single strand of overgrown shish within the sample were extracted from the sample by hot xylene (ca. 110 °C for iPP and 100 °C for PE) using the difference of dissolution temperature of shish and unoriented small crystal.

2.2. Instruments

Crystallization under shear flow and quiescent state was observed by using a hotstage (Linkam, CSS-450). The geometry of the hotstage is parallel plate (bottom plate is rotating). The range of $\dot{\gamma}$ and the gap between both plates h were 0–5 s^{-1} and 100 μm, respectively. Observation of crystallization behavior was carried out by means of a polarizing optical microscope. In order to generate the shish effectively, we set up the salient (small pins: a few micrometers) made from epoxy resin on the top surface (fixed surface) of the parallel plate. These pins will induce the formation of the oriented melt. We can consider that along the flow direction in the neighborhood of the pins the polymer chains are elongated and the oriented melt is formed stationary during the applying of shear flow.

SAXS and WAXD measurements using the synchrotron radiation were performed at the BL40B2 in the SPring-8 (Harima) with approval of the Japan Synchrotron Radiation Research Institute (JASRI) and the BL10C in the Photon Factory (KEK; Tsukuba).

2.3. Measurements

We measured the ΔT dependence of I_{sp} and I_{sh} from the melt under shear flow and quiescent state defined as below. It is noted that before observation of the nucleation all the samples were first melted and annealed at a temperature above T_m^0 ('melt annealing temperature', $T_{max} = 230$ °C for iPP and 160 °C for PE) for 5 min. The T_m^0 of PE under shear flow and quiescent state were almost the same as shown in our previous paper [8]. Therefore, we assumed that T_m^0 of iPP under shear flow and quiescent state are also the same. The ranges of ΔT were 39.1–58.6 K for iPP and 8.3–14.3 K for PE, respectively. We measured the number density of spherulites and shish within the melt. As mentioned in our previous paper, [29] the number density of spherulites (ν_{sp}) should correspond to that of nuclei. In this paper, we assumed the number density of shish (ν_{sh}) should also correspond to that of nuclei. A single nucleus will grow to a shish in earlier stage and then the shish will change to a strand structure via overgrowth. This is an analogy of the formation of a spherulite. This assumption will be confirmed in this paper. We observed a single shish by means of polarizing optical microscope in earlier stage and a strand by WAXD which is formed later stage. Therefore, the number density of nucleus ν was estimated from ν_{sp} and ν_{sh}. I is obtained by

$$\begin{aligned} I \equiv I_{sp} &= d\nu_{sp}/dt \text{ for spherulite} \\ &\equiv I_{sh} = d\nu_{sh}/dt \text{ for shish} \end{aligned} \quad (4)$$

In this work, we abbreviate the above processes to spherulite (Q), spherulite (F) and shish (F), respectively, where Q and F in parenthesis mean quiescent and flow, respectively.

3. Results

3.1. SAXS and WAXD pattern of shish

The single strand of shish as shown in Fig. 4(A) was put on the sample holder along the vertical axis. The length and cross sectional diameter of single strand of shish are 1 mm and 20 μm, respectively. It is noted here that the samples used in X-ray experiments were obtained by extraction of quenching samples consisted of a lot of isolated 'overgrown' shish. Therefore, our X-ray experiments

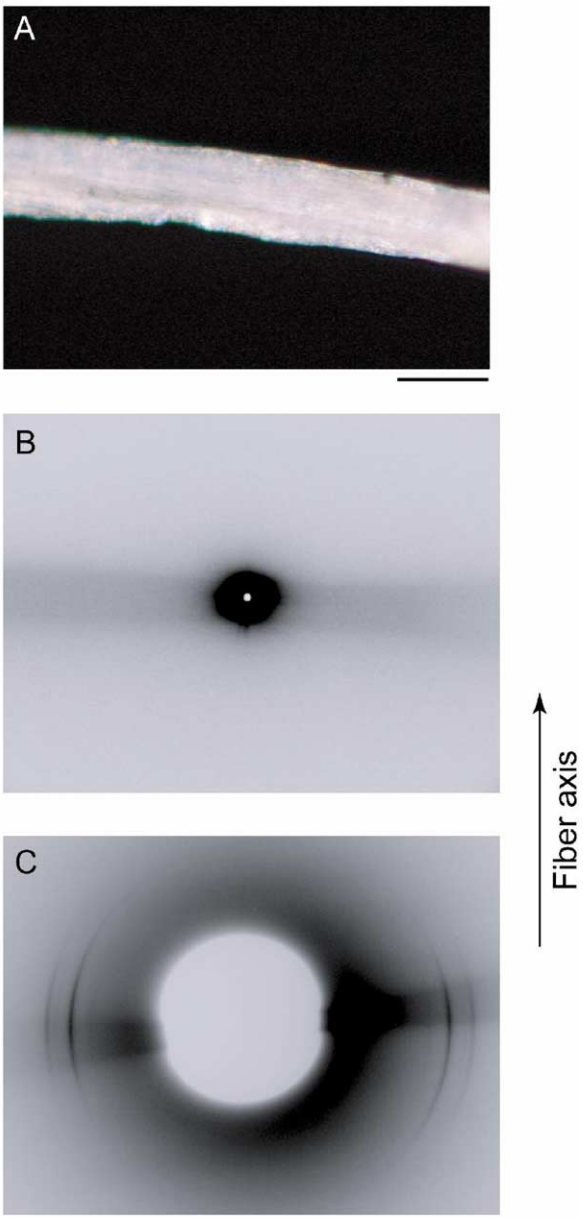

Fig. 4. (A) Polarizing optical micrograph of sample used in X-ray experiments. Scale bar is 20 μm. (B) Two dimensional SAXS pattern of shish of PE after extraction. (C) Two dimensional WAXD pattern of shish of PE after extraction.

should correspond to the observation of fibril sample consisted of a lot of overgrown shish. Fig. 4(B) and (C) show the SAXS and WAXD pattern of shish of PE. In SAXS pattern, we cannot observe any long period. The diffused scattering in the equatorial region is due to slit window of the sample holder. This indicates that the shish after extraction does not have any stacked lamellar structure along the fiber axis. When the cold drawn samples of PE or iPP will be annealed at $T > 100$ °C, long-period reflections can be observed. As the crystallization temperature T_c of shish is much higher than 100 °C, lack of long period indicates that the strand (assembled structure of shish) should be composed of ECCs. In WAXD pattern, on the other hand, we found typical fiber pattern. The 110 and 200 reflections were observed on the equatorial line. The arc appeared in these reflections may be due to the extraction. This indicates that the shish is the oriented crystal in the chain axis (*c* axis). Therefore, we concluded that the shish is consisted of the ECC.

3.2. Shish was formed from bundle nucleus

In this work, we have shown a direct evidence that the bundle nucleus is formed from the oriented melt and it grows to the shish. First, we will show that the shish is effectively formed from the oriented melt caused by pins. The shish was always generated on the root of pins in our experiment and grew to the flow direction. It will be confirmed to show that ν_{sh} increased with increase of the number density of pin ν_{pin}. Second, we will show that the formation of shish is the nucleation with bundle nucleus by confirming the ΔT dependence of I_{sh}. Third, we will propose the universal mechanism of the formation of shish and spherulite under shear flow. The bundle and fold nuclei will be formed from the oriented and isotropic melt and they will grow to the shish and spherulite, respectively.

3.2.1. *t* dependence of ν_{sh}

Fig. 5 shows that ν_{sh} linearly increased with increase of *t*. As well as I_{sp} in the quiescent state, [8,29,30] we can obtain I_{sh} from the slope of this straight line. Moreover, we can define the apparent induction time τ as the intercept of horizontal axis. In the entire T_c in this work, we observed that ν_{sh} for both iPP and PE are the same behavior.

3.2.2. I_{sh} increased with increase of ν_{pin}

Fig. 6 shows typical polarizing optical micrographs of

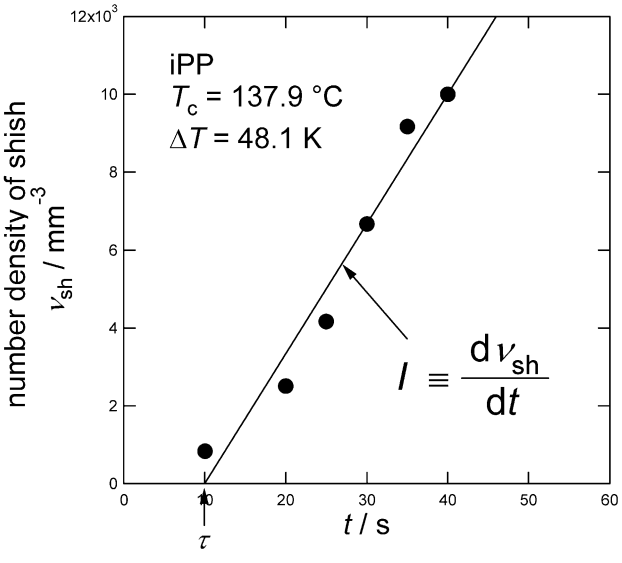

Fig. 5. Plots of ν_{sh} of iPP against *t* at $\Delta T = 48.1$ K. *I* and τ are defined by the slope of the straight line and the intercept of horizontal axis.

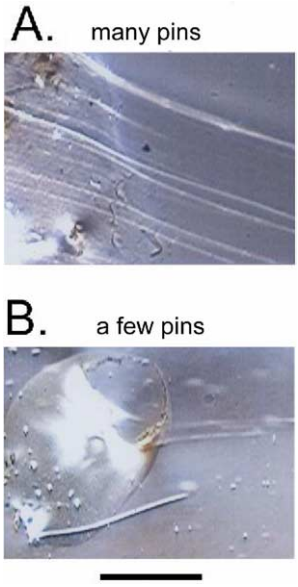

Fig. 6. Typical polarizing optical micrographs of the effect of ν_{pin} on ν_{sh}. Scale bar is 200 μm.

the formation of shish from pins on the surface of upper plate at $\dot{\gamma} = 5\ s^{-1}$. It is obvious that ν_{sh} increased with increase of ν_{pin}. As shown in Fig. 7, we quantitatively found that ν_{sh} significantly increased with increase of ν_{pin}. From this experimental fact, we confirmed our proposed model that the shish is formed from the elongated chains within the oriented melt.

We also found that the melting temperature T_m of shish of PE under very slow heating such as 0.2 °C/min is much higher than that of FCCs and is close to T_m^0 [8]. This indicates that lamellar thickness of crystals is much thicker than that of folded chain crystal (FCC). Therefore, it is reasonable to conclude that the shish consists of ECC.

3.2.3. ΔT dependence of I_{sh} and rate determining process

Fig. 8 shows a typical example of ΔT dependence of $\nu_{sh}(t)$ of PE. We found that the slope of the straight line in Fig. 8 increased with increase of ΔT. This implies that $I(\Delta T)$ increases with increase of ΔT. Moreover, we also found that τ decreased with increase of ΔT. Though the results of iPP was not shown, the results of iPP is almost the same as that of PE.

Figs. 9(A) and 10(A) show the plots of I against ΔT^{-2} from the oriented and isotropic melt (indicated by shish (F) and spherulite (Q and F)) for iPP and PE, respectively. Both iPP and PE, the I from the oriented melt, i.e. the formation of shish obeyed Eq. (1), except for large ΔT of PE. Therefore, we concluded that the formation of shish is controlled by the nucleation process. In large ΔT of PE, it is considered that the formation of shish is controlled by the diffusion, i.e. the chain rearrangement. As mentioned in discussion, we also found that ΔG^* in the case of shish (F) is larger than kT. This also implies that the formation of shish is the nucleation process [23,24]. Since the slope of the straight line of shish (F) was smaller than that of spherulite (Q or F), this indicates that the nucleation mechanism of shish (F) is quite different with that of spherulite (Q and F). Here, it is noted that absolute value of I_0 is not so important because I_0 is proportional to ν_{pin}, i.e. number density of heterogeneity ν_{het} [29,30].

3.2.4. Experimental evidence of the formation of bundle nucleus from the oriented melt

We obtained C of shish (F) (C_{sh}) for iPP and PE as follows,

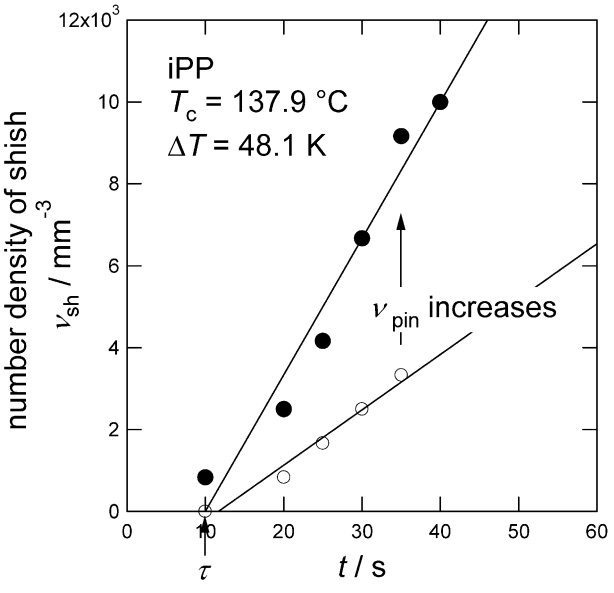

Fig. 7. Plots of ν_{sh} of iPP against t at the same $\Delta T = 48.1$ K. The slope I increased with increase of ν_{pin}.

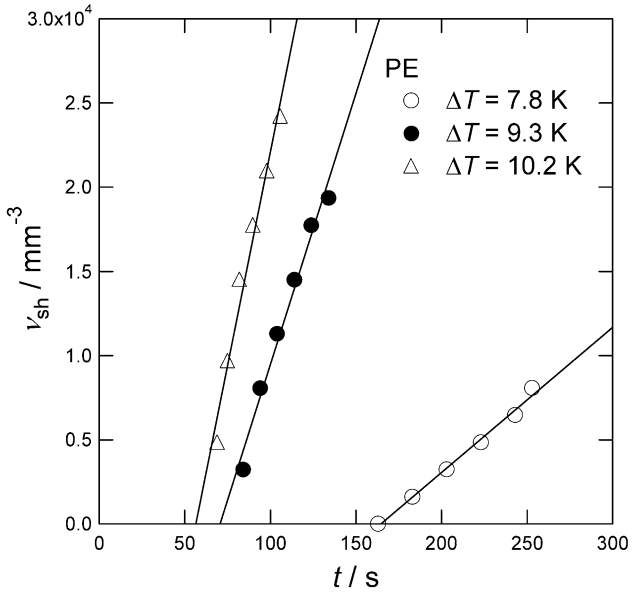

Fig. 8. Plots of ν_{sh} of PE against t at $\Delta T = 7.8$, 9.3 and 10.2 K. The slope I increased with increase of ΔT.

$$C_{sh} = 5.48 \times 10^3 \text{ K}^2 \quad \text{for iPP,}$$
$$= 229 \text{ K}^2 \quad \text{for PE.} \tag{5}$$

As mentioned in Section 1.5, we can judge the type of nucleus from ΔG^* obtained by kinetic observation based on the classical nucleation theory [17]. If the observed σ_e^b is much smaller than σ_e^f, the type of nucleus should be bundle. In the case that the fold nucleus with sharp folds is homogeneously formed from the isotropic melt, we can theoretically calculate C_{homo} as 25×10^4 and 21×10^4 K^2 for iPP and PE, respectively. Therefore, we obtained $C_{sh}/C_{homo} = 2.2\times10^{-2}$ and 1.1×10^{-3} for iPP and PE, respectively [17,26,27,31–34]. Using σ_e^f in the literatures [26,27,31–33] and σ^{ori} shown in part 2 of this series of paper [25], we estimated σ_e^b and summarized in Table 1. Moreover, the parameters used in calculation in this series of paper are summarized in Table 2. From these values, it was directly confirmed that the shish was formed from the bundle nucleus within the oriented melt.

3.2.5. ΔT dependence of I from the isotropic melt

We already showed that I from the isotropic melt under shear flow and quiescent state as shown in Figs. 9A and 10A (indicated by spherulite (F) and spherulite (Q), respectively). For both iPP and PE, I obeyed Eq. (1). The I of spherulite (F) is almost coincident with that of spherulite (Q) at the same ΔT within the experimental errors [30]. Since the slope of the straight lines C and intercept of vertical axis I_0 are almost the same both under shear flow and quiescent state, D and ΔG^* in Eq. (1) are almost the same both under shear flow and quiescent state. The former means that in quasi-isotropic melt the number of clusters related to the local order does not change by shear flow. The latter means that even in the quasi-isotropic melt folded nucleus should be formed as well as in the isotropic melt under quiescent state. From these results, we concluded that the mechanism of nucleation from the quasi-isotropic melt is essentially the same as that from the isotropic melt since the most chains within the sheared melt can be regarded as the ellipsoidal random coiled chains [9,10] and the chain conformation under shear flow is almost the same as that under quiescent state [8].

3.2.6. Induction periods under shear flow

Fig. 11(A) and (B) show the plots of τ of shish (F) and spherulite (F and Q) for iPP and PE against ΔT^{-2}, respectively. Both iPP and PE, it was found that the logτ of shish (F) and spherulite (Q and F) is proportional to ΔT^{-2}. The slopes of the straight line of shish (F) is smaller than that of spherulite (Q and F). This indicates that the molecular mechanism in induction period is quite different between the formation of shish and spherulite. If τ will be measured by more sensitive tools such as SAXS [38], τ should ultimately become to be zero. τ in this work was obtained for a crystal with micrometer order of lateral size.

Table 2
The parameters used in this series of paper

	iPP	PE
Δh (J m^{-3}) [26,35]	1.7×10^8	2.8×10^8
T_m^0 (°C) [31–33,36]	186.1	140.0
a_0 (Å)	6.28	4.55
b_0 (Å)	5.43	4.15
c_0 (Å)	2.17	1.27

a_0, b_0 and c_0 mean the length of repeating unit in unit cell [26,35,37]. The crystal forms are α2 and orthorhombic for iPP and PE, respectively. Fold surface is assumed to be (110).

3.3. Critical shear rate $\dot{\gamma}^*$ for the formation of shish

In this work, we found for the first time that $\dot{\gamma}^*$ for the formation of shish exists. I_{sh} gradually increased with increase of $\dot{\gamma}$, whereas τ rapidly decreased and saturated with increase of $\dot{\gamma}$. Based on these experimental facts, we will show the relation between the elongation and relaxation of chains on the formation of shish.

3.3.1. $\dot{\gamma}$ dependence of $\nu_{sh}(t)$

Fig. 12 shows the $\dot{\gamma}$ dependence of $\nu_{sh}(t)$ of iPP. Below $\dot{\gamma} = 0.1$ s^{-1}, we cannot observe the formation of shish. Above $\dot{\gamma} = 0.5$ s^{-1}, we found that the shish was formed. The slopes of the straight lines, i.e. I_{sh} gradually increased with increase of $\dot{\gamma}$, whereas τ decreased with increase of $\dot{\gamma}$. This implies that $\dot{\gamma}^*$ exists for the formation of shish.

3.3.2. $\dot{\gamma}^*$ of I_{sh} and τ

Fig. 13 shows the $\dot{\gamma}$ dependence of I_{sh} and τ of iPP. We found that I_{sh} gradually increased with increase of $\dot{\gamma}$. Whereas, τ rapidly decreased and then saturated with increase of $\dot{\gamma}$ and diverged to infinity with decrease of $\dot{\gamma}$. The induction periods for the formation of shish strongly

Table 1
The side and end surface free energy of bundle and fold nucleus (unit in J/m^2)

	Side surface free energy		End surface free energy	
	Oriented melt, σ^{ori} [a]	Isotropic melt, σ^{iso} [b]	Bundle nucleus, σ_e^b	Fold nucleus[c], σ_e^f
iPP	6.5×10^{-3}	12×10^{-3}	3.1×10^{-3}	45×10^{-3}
PE	2.6×10^{-3}	14×10^{-3}	3.0×10^{-3}	91×10^{-3}

[a] σ^{ori} was obtained by the growth rate of shish V. The details are presented in our sequential paper [25].
[b] Data taken from Refs. 26 and 34 for PE and iPP, respectively.
[c] Data taken from Refs. 27 and 31–33 for PE and iPP, respectively.

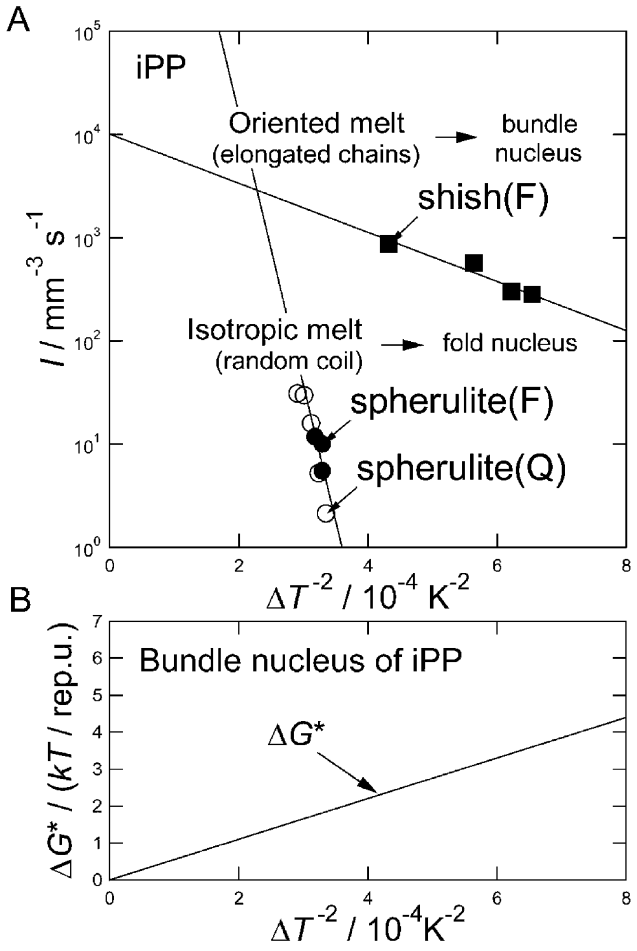

Fig. 9. (A) Plots of I from the oriented and isotropic melt of iPP against ΔT^{-2}. The solid lines obeyed the classical nucleation theory (Eq. (1)). The slope of the straight line of shish (F) is smaller than that of spherulite (F and Q). (B) ΔT dependence of ΔG^* of the bundle nucleus of iPP.

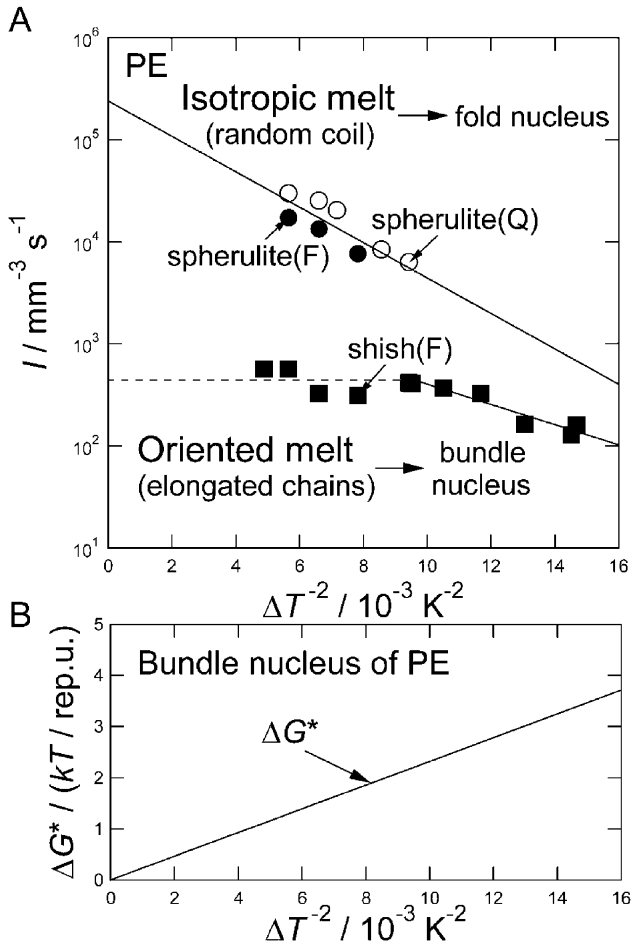

Fig. 10. (A) Plots of I from the oriented and isotropic melt of PE against ΔT^{-2}. The solid lines obeyed the classical nucleation theory (Eq. (1)). The slope of the straight line of shish (F) is smaller than that of spherulite (F and Q). (B) ΔT dependence of ΔG^* of the bundle nucleus of PE.

depends on $\dot{\gamma}$. As shown in this figure, we can clearly define $\dot{\gamma}^*$ for the formation of shish as

$$\dot{\gamma}^* \approx 0.5\ \mathrm{s}^{-1} \tag{6}$$

4. Discussion

4.1. Bundle nucleus was formed from the oriented melt

From the experimental facts, we have proposed the model of chain conformation under shear flow. The chain conformation within the sheared melt becomes to be ellipsoidal random coils [9,10]. When a part of the chains will be accidentally elongated by the dust particles or pins within the melt, the oriented melt will be formed and then the bundle nucleus will grow to the shish. We have shown based on kinetic study that the fold and bundle nucleus are formed from the isotropic and the oriented melt, respectively. Since the ΔG^* of a bundle nucleus is much smaller than that of a fold nucleus, the nucleation of bundle nucleus is much easier than that of fold nucleus. This is the reason why the nucleation behavior under flow is significantly different from that under quiescent state. For polymers, it has confirmed that our proposed model of nucleation as shown in Fig. 3 is universal.

4.2. Reason why $\dot{\gamma}^*$ exists for the formation of shish

Let us consider the reason why $\dot{\gamma}^*$ exists for the formation of shish. Fig. 14 shows a schematic illustration of the relation between the size of a critical bundle nucleus (l^*) and length of elongated chain (L) near $\dot{\gamma}^*$. Under the shear flow, the elongated chains caused by pin will relax to the random coils as shown in Fig. 14(C). Competition of these two factors, i.e. elongation and relaxation controls L. As was mentioned previously, since the shish was always generated on the root of pins, the bundle nucleus should be formed on the root of pins. If $L \gg l^*$, it is possible to progress the nucleation. On the other hand, if $L \ll l^*$, the

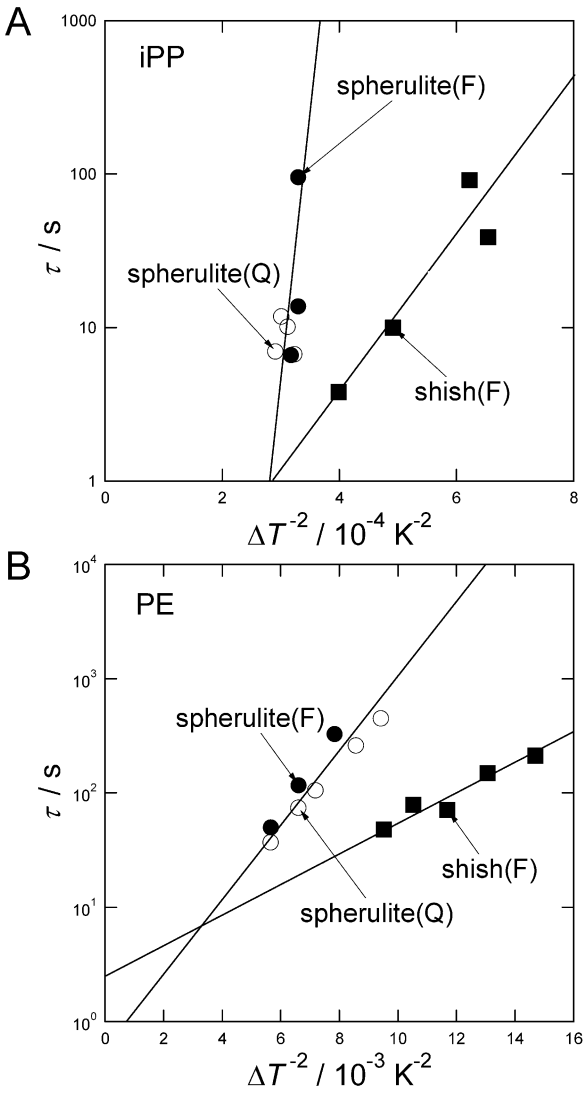

Fig. 11. Plots of τ of shish (F) and spherulite (F and Q) against ΔT^{-2} of (A) iPP and (B) PE.

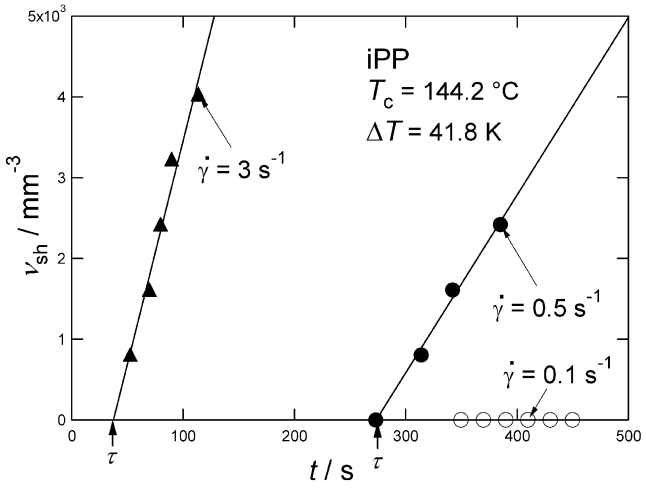

Fig. 12. Plots of ν_{sh} of iPP against t in $\dot{\gamma} = 0.1, 0.5$ and 3 s^{-1} at $\Delta T = 41.8$ K. The slope I increased with increase of $\dot{\gamma}$.

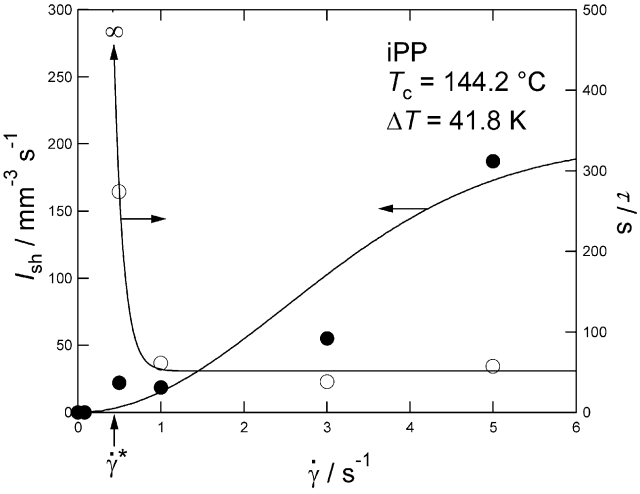

Fig. 13. Plots of I and τ of shish (F) of iPP against $\dot{\gamma}$ at $\Delta T = 41.8$ K.

nucleation can not progress. This is the reason why $\dot{\gamma}^*$ exists for the formation of shish. It is noted here that $\dot{\gamma}^*$ may depend on the variety of polymer.

4.3. ΔT dependence of ΔG^* and shape of the critical bundle nucleus

Using obtained σ^{ori} and σ_e^b, we can calculate ΔG^* of

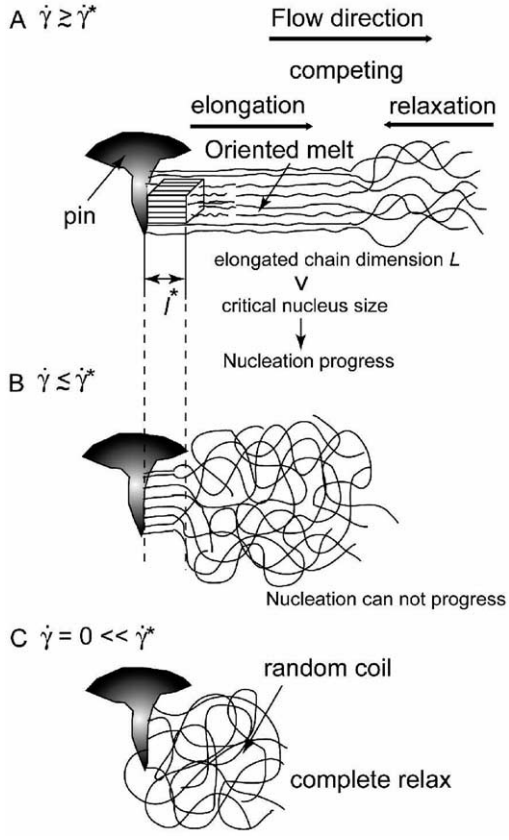

Fig. 14. Schematic illustration of the conformation of elongated chains caused by pin at (A) $\dot{\gamma} > \dot{\gamma}^*$, (B) $\dot{\gamma} < \dot{\gamma}^*$ and (C) $\dot{\gamma} = 0 \ll \dot{\gamma}^*$.

bundle nucleus against ΔT^{-2} as shown in Figs. 9(B) and 10(B):

$$\begin{aligned}\Delta G^* &= 5.5\times10^3/\Delta T^2\ (kT/\text{rep.unit}) \quad \text{for iPP}\\ &= 2.3\times10^2/\Delta T^2\ (kT/\text{rep.unit}) \quad \text{for PE}\end{aligned} \tag{7}$$

In a range of ΔT except for large ΔT of PE, we concluded that the formation of shish is mainly controlled by the nucleation process since a criterion that $\Delta G^* > 2\,kT$ was satisfied. At $\Delta T \sim 10.3$ K of PE, i.e. $\Delta G^* \sim 2\,kT$, there is a breaking point on the plot of I against ΔT^{-2}. Therefore, in the case of $\Delta T > 10.3$ K of PE, it is controlled by the diffusion process.

We can calculate the size of critical bundle nucleus, i.e. l^*, m^* and n^* as

$$\begin{aligned}l^* &= 1.6\times10^2/\Delta T\ (\text{rep.unit}) \quad \text{for iPP}\\ &= 1.4\times10^2/\Delta T\ (\text{rep.unit}) \quad \text{for PE}\end{aligned} \tag{8}$$

$$\begin{aligned}m^* = n^* &= 130/\Delta T\ (\text{rep.unit}) \quad \text{for iPP}\\ &= 35/\Delta T\ (\text{rep.unit}) \quad \text{for PE}\end{aligned} \tag{9}$$

where we assumed that $m^* = n^*$ for the critical bundle nucleus [17].

The shape of critical bundle nucleus is assumed to be rectangular solid. l^*, m^* or n^* are a few to several tens nm in the range of ΔT in this work. It was found that l^* of the bundle nucleus is much smaller than that of the fold nucleus ($l^* = 4.3\times10^3/\Delta T$ for PE).

5. Conclusion

1. The formation of shish is mainly controlled by the nucleation process of the bundle nucleus except for large ΔT.
2. The bundle and fold nuclei were formed from the oriented and isotropic melt, respectively.
3. There exists a critical shear rate $\dot{\gamma}^*$ for the formation of shish. $\dot{\gamma}^* \approx 0.5\ \text{s}^{-1}$ for iPP.

Acknowledgements

This work was partly supported by Grant-in-Aid for JSPS Fellow (No. 08115) and Scientific Research on Priority Areas B2 (No. 12127205) and Scientific Research A2 (No. 12305062) from the Ministry of Education, Culture, Sports, Science and Technology, Japan. The synchrotron radiation experiments were performed at the BL40B2 in the SPring-8 (Harima) with approval of the Japan Synchrotron Radiation Research Institute (JASRI) and the BL10C in the Photon Factory (KEK; Tsukuba).

References

[1] Pennings AJ. J Polym Sci, Polym Symp 1977;59:55–86.
[2] Pennings AJ, van der Mark JMAA, Booij HC. Kolloid Z. Z. Polymere 1969;236:99–111.
[3] Pennings AJ, van der Mark JMAA, Kiel AM. Kolloid Z. Z. Polymere 1970;237:336–58.
[4] Andrews EH, Owen PJ, Singh A. Proc Roy Soc Lond A 1971;324:79–97.
[5] Bassett DC. Principles of polymer morphology. Cambridge: Cambridge University Press; 1981.
[6] Mackley MR, Keller A. Philos Trans R Soc London, Ser A 1975;278:29–66.
[7] Keller A, Odell JA. Colloid Polym Sci 1985;263:181–201.
[8] Yamazaki S, Hikosaka M, Toda A, Wataoka I, Yamada K, Tagashira K. J Macromol Sci, Phys 2003;B42:499–514.
[9] Lindner P, Oberthür RC. Colloid Polym Sci 1985;263:443–53.
[10] Muller R, Pesce JJ, Picot C. Macromolecules 1993;26:4356–62.
[11] Frank FC. Proc Roy Soc Lond A 1970;319:127–36.
[12] De Gennes PG. J Chem Phys 1974;60:5030–42.
[13] Xu G, Ding J, Yang Y. J Chem Phys 1997;107:4070–84.
[14] Dukovski I, Muthukumar M. J Chem Phys 2003;118:6648–55.
[15] Hikosaka M. Polymer 1987;28:1257–64.
[16] Hikosaka M. Polymer 1990;31:458–68.
[17] Price FP. Nucleation in polymer crystallization. In: Zettlemoyer AC, editor. Nucleation. New York: Marcel Dekker; 1969. Chapter 8.
[18] Wunderlich B, Arakawa T. J Polym Sci 1964;2:3697–706.
[19] Hikosaka M, Amano K, Rastogi S, Keller A. Macromolecules 1997;30:2067–74.
[20] Hikosaka M, Amano K, Rastogi S, Keller A. J Mater Sci 2000;35:5157–68.
[21] Hoffman JD. Polymer 1979;20:1071–7.
[22] Flory PJ. Principles of polymer chemistry. Ithaca: Cornell University Press; 1953.
[23] Becker R, Döring W. Ann Phys 1935;24:719–52.
[24] Turnbull D, Fisher JC. J Chem Phys 1949;17:71–3.
[25] Yamazaki S, Hikosaka M, Toda A, Okada K, Das NC, Watanabe K, Yamada K, Tagashira K. Polymer, 2005, this issue (Part 2).
[26] Hoffman JD, Frolen LJ, Ross GS, Lauritzen Jr JI. J Res NBS 1975;79A:671–99.
[27] Corradini P, Petraccone V, Allegra G. Macromolecules 1971;4:770–1.
[28] Hoffman JD, Lauritzen Jr JI. J Res NBS 1961;65A:297–336.
[29] Nishi M, Hikosaka M, Ghosh SK, Toda A, Yamada K. Polym J 1999;31:749–58.
[30] Ghosh SK, Hikosaka M, Toda A, Yamazaki S, Yamada K. Macromolecules 2002;35:6985–91.
[31] Yamada K, Hikosaka M, Toda A, Yamazaki S, Tagashira K. Macromolecules 2003;36:4790–801.
[32] Yamada K, Hikosaka M, Toda A, Yamazaki S, Tagashira K. Macromolecules 2003;36:4802–12.
[33] Yamada K, Hikosaka M, Toda A, Yamazaki S, Tagashira K. J Macromol Sci 2003;B42:733–52.
[34] Cheng SZD, Janimak JJ, Zhang A, Cheng HN. Macromolecules 1990;23:298–303.
[35] Brandrup J, Immergut EH, Grulke EA. Polymer handbook. 4th ed. New York: Wiley; 1999.
[36] Okada M, Nishi M, Takahashi M, Matsuda H, Toda A, Hikosaka M. Polymer 1998;39:4535–9.
[37] Hikosaka M, Seto T. Polym J 1973;5:111–27.
[38] Hikosaka M, Yamazaki S, Wataoka I, Das NC, Okada K, Toda A, Inoue K. J Macromol Sci, Phys 2003;B42:847–65.